Supplementary Tables and Figures

Supplementary Table 1. Significant clusters within the neural threat-predictive pattern. Related to Figure 2A

		MNI Coordinates					
	Region	x	y	z	voxels	mm3	max stat
Cortex							
Frontal Lobe							
R	Inferior Frontal Gyrus	48	26	-18	1	8	-3.73
L	Middle Frontal Gyrus	-38	52	-10	256	2048	-5.73
R	Middle Frontal Gyrus	32	36	46	8	64	-3.92
R	Superior Frontal Gyrus	38	48	20	5	40	-3.90
R	Superior Frontal Gyrus	40	34	30	18	144	-4.56
L	Anterior Cingulate	-14	42	6	1	8	3.70
L	Cingulate Gyrus	-4	8	40	1	8	3.73
Temporal Lobe							
R	Insula	42	-16	14	4	32	3.80
L	Fusiform Gyrus	-44	-54	-8	12	96	4.17
R	Inferior Temporal Gyrus	28	-12	-42	7	56	3.94
		64	-14	-20	2	16	-3.84
R	Inferior Temporal Gyrus	64	-52	-18	7	56	4.27
L	Middle Temporal Gyrus	-52	-68	24	20	160	-4.13
		-62	-32	-12	2	16	-3.71
R	Middle Temporal Gyrus	54	-2	-8	9	72	-4.13
		66	-26	-4	4	32	-3.81
L	Superior Temporal Gyrus	-50	-2	6	1	8	3.70
		-48	-48	10	1	8	3.70
R	Parahippocampal Gyrus	12	-16	-16	2	16	3.96
L	Parahippocampal Gyrus	-24	-46	-4	4	32	4.23
R	Amygdala	24	-4	-6	11	88	4.03
Parietal Lobe							
L	Inferior Parietal Lobule	-48	-66	40	106	848	-4.85
R	Postcentral Gyrus	54	-24	22	13	104	4.41
L	Precuneus	-32	-64	36	1	8	-3.83
R	Precuneus	14	-58	42	1	8	-3.79
R	Superior Parietal Lobule	14	-56	64	47	376	-4.35
Occipital Lobe							

R	Cuneus	16	-76	10	4	32	4.02
SubCortex							
L	Basal Ganglia:Globus Pallidus	-12	0	-6	14	112	4.36
L	Thalamus: Ventral Anterior Nucleus	-8	-4	8	7	56	4.28
Cerebellum							
L	Cerebellum, Declive	-6	-74	-18	99	792	5.91
		-8	-60	-18	32	256	4.12
B	**Midbrain**						
L	Periacqueductal Gray	-2	-26	-6	204	1632	6.04
R	Substania Nigra	12	-18	-12	3	24	3.93

* Thresholded (bootstrapped 5,000 samples) and corrected for multiple comparisons (FDR $p < 0.05$, k = 1)

Supplementary Table 2. Significant clusters in univariate acquisition (CS+>CS-) map. Related to STAR METHODS QUANTIFICATION AND STATISTICAL ANALYSIS *Univariate Analysis* and Figure S1

	Region	MNI Coordinates x	y	z	voxels	mm3	maxstat
Cortex							
Frontal Lobe							
L	Medial Frontal Gyrus	-10	56	-14	75	600	-4.08
		-38	54	-8	753	6024	-5.01
L	Middle Frontal Gyrus	-42	18	42	51	408	-3.76
		-58	26	28	8	64	-3.41
L	Premotor Cortex	-10	-26	46	12	96	3.89
L	Orbitofrontal Cortex	-6	42	-28	17	136	-3.6
		-4	30	18	63	504	4.48
L	Anterior Cingulate Gyrus	-2	24	24	356	2848	4.92
		-20	22	24	33	264	4.37
		-4	8	40	427	3416	6.2
R	Middle Frontal Gyrus	58	44	-8	6	48	-3.38
R	Inferior Frontal Gyrus	36	20	-6	206	1648	4.2
R	Superior Frontal Gyrus	20	48	38	6	48	-3.43
R	Precentral Gyrus	34	-22	48	26	208	3.73
		48	-12	48	19	152	3.43
R	Mid Cingulate Gyrus	6	-20	28	9	72	3.51
R	Anterior Cingulate Gyrus	8	-22	44	109	872	4.15
		6	2	42	461	3688	6.53
Temporal Lobe							
L	Middle Temporal Gyrus	-60	-30	-12	685	5480	-5.73
		-38	-20	16	44	352	3.95
		-36	10	2	285	2280	4.94
L	Insula	-36	0	-6	116	928	4.1
		-30	20	8	417	3336	6.05
		-40	0	10	616	4928	6.65
L	Superior Temporal Gyrus	-56	2	6	146	1168	5.48
L	Transverse Temporal Gyrus	-52	-22	12	290	2320	5.15
L	Fusiform Gyrus	-40	-52	-6	14	112	7.82
R	Middle Temporal Gyrus	66	-20	-18	276	2208	-5.29
		58	-36	20	119	952	4.42
R	Insula	36	-22	18	153	1224	5.12
		48	-18	16	250	2000	5.24

		38	-10	-2	81	648	4.23
		36	-16	10	104	832	4.21
R	Superior Temporal Gyrus	48	-58	28	90	720	-4.19
		56	-2	4	61	488	4.61
R	Amygdala	22	-14	-8	69	552	4.43
Parietal Lobe							
		-46	-66	40	1337	10696	-5.98
L	Inferior Parietal Lobule	-56	-28	24	627	5016	6.72
		-50	-38	22	123	984	4.48
L	Precuneus	0	-60	36	99	792	-3.75
R	Inferior Parietal Lobule	56	-26	22	303	2424	6.46
		50	-32	24	86	688	4.62
R	Superior Parietal Lobule	40	-68	52	36	288	-3.91
R	Angular Gyrus	38	-62	34	14	112	-3.69
Occipital Lobe							
L	Middle Occipital Gyrus	-38	-92	14	30	240	-4.13
SubCortex							
L	Caudate	-14	-12	20	6	48	3.37
L	Lentiform Nucleus	-14	4	-6	476	3808	7.82
R	Caudate	10	10	2	232	1856	4.16
R	Lentiform Nucleus	24	2	-4	251	2008	5.34
R	Nucleus Accumbens	22	12	-12	232	1856	4.32
R	Claustrum	32	6	8	391	3128	5.72
R	Thalamus: Medial Dorsal Nucleus	6	-18	10	83	664	3.97
Cerebellum							
L	Cerebellum, Culmen	-28	-50	-28	147	1176	5.01
		-6	-56	-14	171	1368	4.83
L	Cerebellum, Declive	-6	-70	-18	77	616	4.39
R	Cerebellum, Culmen	4	-58	-28	27	216	3.66
		40	-50	-32	26	208	3.7
R	Cerebellum, Anterior Lobe	2	-46	-16	5	40	3.34
		2	-48	-12	16	128	3.62
Brainstem							
L	Midbrain, Periacqueductal Gray	-2	-14	-12	356	2848	5.41
R	Pons	8	-34	-42	40	320	4.27
R	Midbrain, Substantia Nigra	10	-20	-12	317	2536	5.79

* Thresholded and corrected for multiple comparisons (FDR $p < 0.05$, k=5)

Supplementary Table 3. Univariate activation during recovery test (CS + > CS-). Related to STAR METHODS QUANTIFICATION AND STATISTICAL ANALYSIS *Univariate Analysis* and Figure S4.

Imagined	Region	MNI Coordinates			voxels	mm3	max stat
		x	y	z			
Cortex							
Temporal Lobe							
R	'Temporal_Inf_R (aal)'	46	-70	-4	284	2272	-5.07
Occipital Lobe							
L	'Calcarine_L (aal)'	-10	-98	-6	111	888	-4.69
L	'Cuneus_L (aal)'	-6	-86	16	234	1872	-5.09
L	Occipital_Mid'	-26	-86	34	191	1528	-4.8
R	Occipital_Mid'	32	-74	32	151	1208	-4.59

Real	Region	MNI Coordinates			voxels	mm3	max stat
		x	y	z			
Cortex							
Frontal Lobe							
R	'Inferior Frontal Gyrus'	48	38	2	43	344	-4.57
R	'Inferior Frontal Gyrus'	58	8	36	80	640	-4.59
R	'Middle Frontal Gyrus'	24	28	-18	108	864	-4.29
R	'Middle Frontal Gyrus'	24	-2	48	98	784	-4.47
Temporal Lobe							
L	Amygdala	-16	-8	-32	120	960	-5.01
R	'Insula'	46	8	12	50	400	-4.43
R	Insula	42	4	24	71	568	-4.73
R	'Fusiform Gyrus'	56	-50	-24	68	544	-4.37
L	'Superior Temporal Gyrus'	-36	0	-20	66	528	-4.32
L	'Superior Temporal Gyrus'	-54	-42	8	76	608	-4.32
R	'Superior Temporal Gyrus'	40	6	-22	75	600	-4.33
L	Hippocampus	-40	-22	-14	52	416	-4.41
Parietal Lobe							
R	'Inferior Parietal Lobule'	56	-38	24	254	2032	-4.85
R	'Parietal_Inf_R (aal)'	32	-46	50	634	5072	-5.01
L	'Postcentral Gyrus'	-58	-24	40	205	1640	-4.52
Occipital Lobe							
L	'Middle Occipital Gyrus'	-32	-82	8	1349	10792	-6.02

	Region	x	y	z	voxels	mm3	max stat
R	'Precuneus'	20	-72	28	2978	23824	-6.19
Cerebellum							
L	'Culmen'	-44	-44	-30	294	2352	-5.56
L	'Declive'	-28	-84	-24	96	768	-5.37
Brainstem							
L	'Pons'	-8	-12	-32	240	1920	-5.01

None	**Region**	**MNI Coordinates**			**voxels**	**mm3**	**max stat**
		x	**y**	**z**			
Cortex							
Frontal Lobe							
L	'Cingulate Gyrus'	-6	-12	30	60	480	5.11
R	'Middle Frontal Gyrus'	32	28	36	50	400	-4.14
L	'Inferior Frontal Gyrus'	-30	32	-4	117	936	5.45
Temporal Lobe							
L	Amygdala	-10	-8	-14	68	544	4.21
L	Hippocampus	-36	-28	-12	80	640	4.62
R	Insula	46	4	20	77	616	-4.19

* Thresholded uncorrected (p < 0.05, k = 5)

Supplementary Table 4. There was no effect of order or stimulus counterbalancing on SCR, Related to Figure 3 and Figure S4

Type III ANOVA with Satterthwaite's method

Source	*df*	*SS*	*MS*	*F*	*P*
Group	2, 60	0.003	0.002	0.325	0.724
Order	1, 60	0.002	0.002	0.355	0.554
Group:Order	2, 60	0.001	0.001	0.128	0.880

Post hoc within group contrasts (all phases): Order A – Order B

Group	*df*	*Estimate*	*SE*	*t.ratio*	*P*
Imagined Extinction	60	-0.001	0.016	-0.042	0.967
Standard Extinction	60	0.010	0.014	0.735	0.465
No Extinction	60	0.006	0.014	0.412	0.682

Within Acquisition Phase (all groups) ANOVA Contrast: Order A – B

	df	*SS*	*MS*	*F*	*P*
Order	1	0.004	0.004	0.256	0.614
Residuals	64	0.885	0.014		

Supplementary Table 5. Post hoc analyses of the neural network supporting imagined extinction. Related to Figure 4D

10 out of 12 nodes yielded group significant differences in betweenness centrality in a one-way ANOVA test, FDR corrected for multiple comparisons.

One-way Analysis of Variance of the Betweenness Centrality of the L NAc Node by Group

Source	*df*	*SS*	*MS*	*F*	*P*	η 2
Between groups	2	18008.8	9004.42	35.17	5.54e-11	0.53
Within groups	63	16131.1	256.05			
Total	65	34139.9				

Significant pair-wise two-sample t-tests with unequal variance:

None > Imagined $t(23) = 8.68$, $P < 0.0001$, CI = [30.92, 50.26], Hedges g = 2.35
None > Real $t(38.39) = 3.03$, $P = 0.004$, CI = [5.56, 27.97], Hedges g = -0.86
Real > Imagined $t(21) = 8.04$, $P < 0.0001$, CI=[17.66, 29.98], Hedges g=2.32

One-way Analysis of Variance of the Betweenness Centrality of the R NAc Node by Group

Source	*df*	*SS*	*MS*	*F*	*P*	η 2
Between groups	2	12522.6	6261.31	21.03	1.01e-07	0.40
Within groups	63	18757.9	297.74			
Total	65	31280.5				

Significant pair-wise two-sample t-tests with unequal variance:

Imagined > None $t(25.42) = 5.79$, $P < 0.0001$, CI = [17.57, 36.93], Hedges g =1.58
Imagined > Real $t(24.17) = 8.13$, $P < 0.0001$, CI = [24.05, 40.40], Hedges g = 2.36

One-way Analysis of Variance of the Betweenness Centrality of the L Amygdala-CM Node by Group

Source	*df*	*SS*	*MS*	*F*	*P*	η 2
Between groups	2	20386.3	10193.2	58.51	4.33e-15	0.65
Within groups	63	10975.5	174.2			
Total	65	31361.8				

Significant pair-wise two-sample t-tests with unequal variance:

Imagined > Real $t(25.8) = 13.59$, $P < 0.0001$, CI = [32.08, 43.53], Hedges g = 3.96
None > Real $t(40.87) = 8.14$, $P < 0.0002$, CI = [27.69, 45.96], Hedges g = 2.32

One-way Analysis of Variance of the Betweenness Centrality of the R Amygdala-CM Node by Group

Source	*df*	*SS*	*MS*	*F*	*P*	η 2
Between groups	2	492.1	246.038	1.59	0.211 *n.s.*	0.04
Within groups	63	9725.2	154.368			
Total	65	10217.3				

** ANOVA not significant; pair-wise t-tests not reported*

One-way Analysis of Variance of the Betweenness Centrality of the L Amygdala-LB Node by Group

Source	*df*	*SS*	*MS*	*F*	*P*	η 2
Between groups	2	225.12	112.56	3.49	0.039 *n.s.*	0.10
Within groups	63	2031.91	32.25			
Total	65	2257.03				

** ANOVA not significant; pair-wise t-tests not reported*

One-way Analysis of Variance of the Betweenness Centrality of the R Amygdala-LB Node by Group

Source	*df*	*SS*	*MS*	*F*	*P*	η 2
Between groups	2	5558	2779.00	17.6	8.44e-07	0.36
Within groups	63	9945.03	157.858			
Total	65	15503.03				

Significant pair-wise two-sample t-tests with unequal variance:

Real > Imagined $t(39.42) = 4.21$, $P = 0.0001$, CI = [9.26, 26.34], Hedges $g = 1.26$
Real > None $t(35.89) = 5.38$, $P < 0.0001$, CI = [12.83, 28.34], Hedges $g = 1.59$)

One-way Analysis of Variance of the Betweenness Centrality of the L Auditory (Te1.0) Node by Group

Source	*df*	*SS*	*MS*	*F*	*P*	η 2
Between groups	2	6524.12	3262.06	761.66	7.36e-45	0.96
Within groups	63	269.82	4.28			
Total	65	6793.94				

Significant pair-wise two-sample t-tests with unequal variance:

Real > Imagined $t(21) = 27.60$, $P < 0.0001$, CI = [19.50, 22.68], Hedges $g = 7.97$
Real > None $t(21) = 27.59$, $P < 0.0001$, CI = [19.50, 22.68], Hedges $g = 8.37$

One-way Analysis of Variance of the Betweenness Centrality of the R Auditory (Te1.0) Node by Group

Source	*df*	*SS*	*MS*	*F*	*P*	η 2
Between groups	2	5551.62	2775.81	45619.84	2.65e-100	1.00
Within groups	63	3.83	0.06			
Total	65	5555.45				

Significant pair-wise two-sample t-tests with unequal variance:

Imagined > Real $t(23) = \text{Inf}$, $P < 0.0001$, CI = [20,20], Hedges $g = \text{Inf}$
Imagined > None $t(23) = 239.00$, $P < 0.0001$, CI = [19.74, 20.01], Hedges $g = 64.74$

One-way Analysis of Variance of the Betweenness Centrality of the L CA1 Node by Group

Source	*df*	*SS*	*MS*	*F*	*P*	η 2
Between groups	2	31964.4	15982.2	251.05	9.71e-31	0.89
Within groups	63	4010.6	63.7			

Total	65	35975

Significant pair-wise two-sample t-tests with unequal variance:

Real > Imagined $t(21.84) = 15.73$, $P < 0.0001$, CI = [40.28, 52.52], Hedges $g = 4.55$
Real > None $t(21.03) = 16.06$, $P < 0.0001$, CI = [40.84, 52.99], Hedges $g = 4.87$

One-way Analysis of Variance of the Betweenness Centrality of the R CA1 Node by Group

Source	*df*	*SS*	*MS*	*F*	*P*	η 2
Between groups	2	2978.95	1489.48	78.75	7.27e-18	0.71
Within groups	63	1191.53	18.91			
Total	65	4170.48				

Significant pair-wise two-sample t-tests with unequal variance:

None > Real $t(23) = 11.48$, $P < 0.0001$, CI = [12.01, 17.31], Hedges $g = 3.18$
Imagined > Real ($t(19) = 15.68$, $P < 0.0001$, CI = [11.87, 15.53], Hedges $g = 4.99$)

One-way Analysis of Variance of the Betweenness Centrality of the PAG Node by Group

Source	*df*	*SS*	*MS*	*F*	*P*	η 2
Between groups	2	3931.62	1965.81	46.95	3.29e-13	0.60
Within groups	63	2637.65	41.87			
Total	65	6569.27				

Significant pair-wise two-sample t-tests with unequal variance:

None > Imagined $t(29.74) = 2.84$, $P = 0.008$, CI = [1.80, 11.04], Hedges $g = 0.88$
None > Real $t(44) = 12.26$, $P < 0.0001$, CI = [15.31, 21.34], Hedges $g = 3.54$
Imagined > Real $t(28.77) = 5.32$, $p < 0.0001$, CI=[7.33, 16.49], Hedges g=1.65

One-way Analysis of Variance of the Betweenness Centrality of the vmPFC Node by Group

Source	*df*	*SS*	*MS*	*F*	*P*	η 2
Between groups	2	19691.5	9845.73	30.79	4.72e-10	0.49
Within groups	63	20148.3	319.81			
Total	65	39839.8				

Significant pair-wise two-sample t-tests with unequal variance:

Imagined > Real $t(25.48) = 4.33$, $P = 0.0002$, CI = [11.05, 31.04], Hedges $g = 1.26$
Imagined > None $t(29) = 9.63$, $P < 0.0001$, CI = [33.41, 51.42], Hedges $g = 2.66$
Real > None $t(42.96) = 3.45$, $P = 0.001$, CI=[8.88, 33.87], Hedges g= 1.00

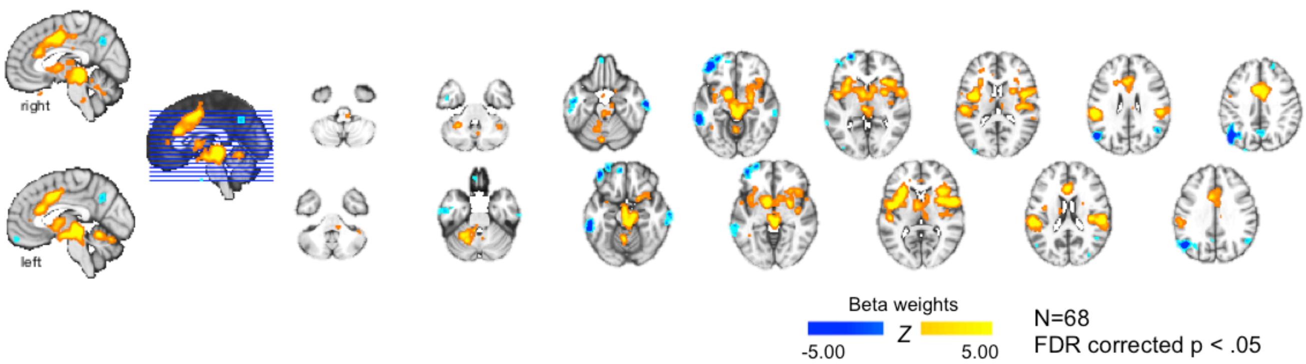

Supplementary Figure 1. Univariate activation during threat Acquisition (CS + > CS-), Related to Figure 2. This the FDR corrected contrast map (CS+ > CS-) resulting from a univariate general linear model applied to all subjects (n = 68) during the Threat Acquisition phase. This map is similar to the multivariate Neural Threat-Predictive Pattern in the main text. Regions with positive activations include the dACC, PAG, amygdala and insula. Regions with negative activations include the precuneus and orbitofrontal cortex. See Table S2 for a detailed list of regions.

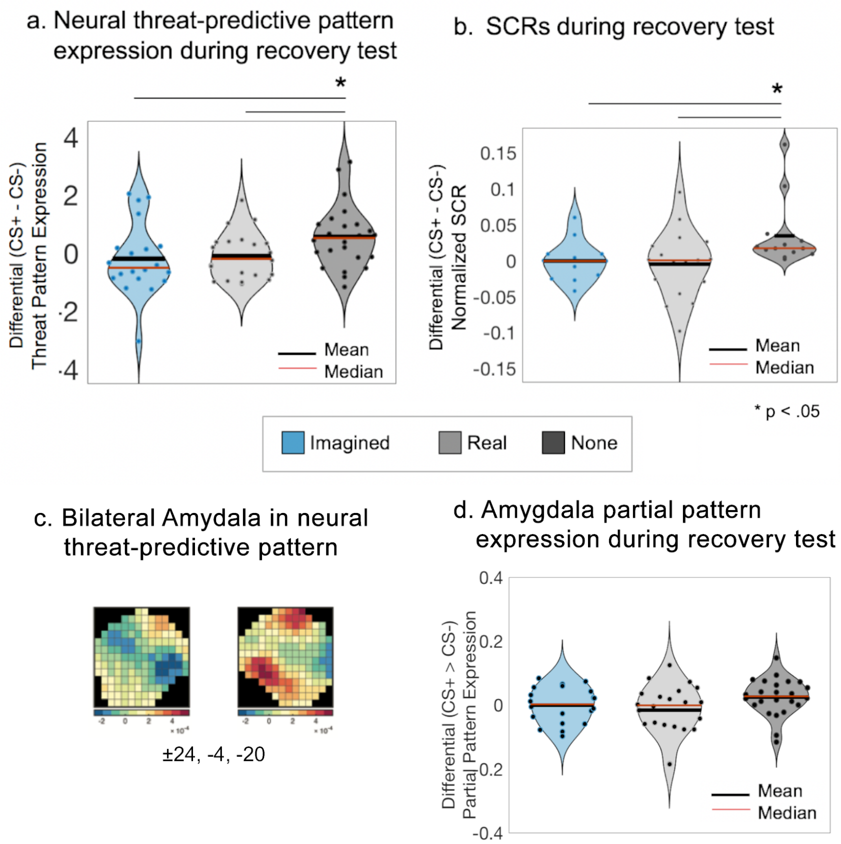

Supplementary Figure 2. Imagined and real extinction reduce neural and physiological threat expression, Related to Figures 2 and 3. A-B. Violin plot version of Figure 3 panels A and B in the main text. See Figure 3 in main text for details. **C.** The unthresholded classification weights in the amygdala extracted from the whole brain threat predictive pattern in Figure 2 of the main text. The neural threat-predictive pattern was masked with a bilateral anatomical mask of the amygdala and then applied to the threat recovery test phase (late re-extinction) in order to determine if threat expression was altered in this region of interest. **D.** The partial threat pattern expression of the amygdala was assessed in the three groups (analogous to Figure 3A). Group differences were not significant, but there is a trend consistent with the findings in this paper: The no extinction group increased threat expression in the amygdala during the recovery test but the imagined and real extinction groups did not ($F(2,63) = 2.35$, p = 0.11, $\eta^2 = 0.07$). The no extinction group ($\underline{x}$ = 0.02, n = 24) is greater than real ($\underline{x}$ = -0.02, n = 22; $t(38.68) = 2.00$, p = 0.05, Hedges g = 0.59), and is non-significantly greater than imagined ($\underline{x}$ = -0.0005, n = 20, $t(41.04) = 1.46$, p = 0.15, Hedges g = 0 .43). No difference was found between the imagined and real ($t(38.10) = 0.75$, p = 0.46, Hedges g = 0.22) extinction groups.

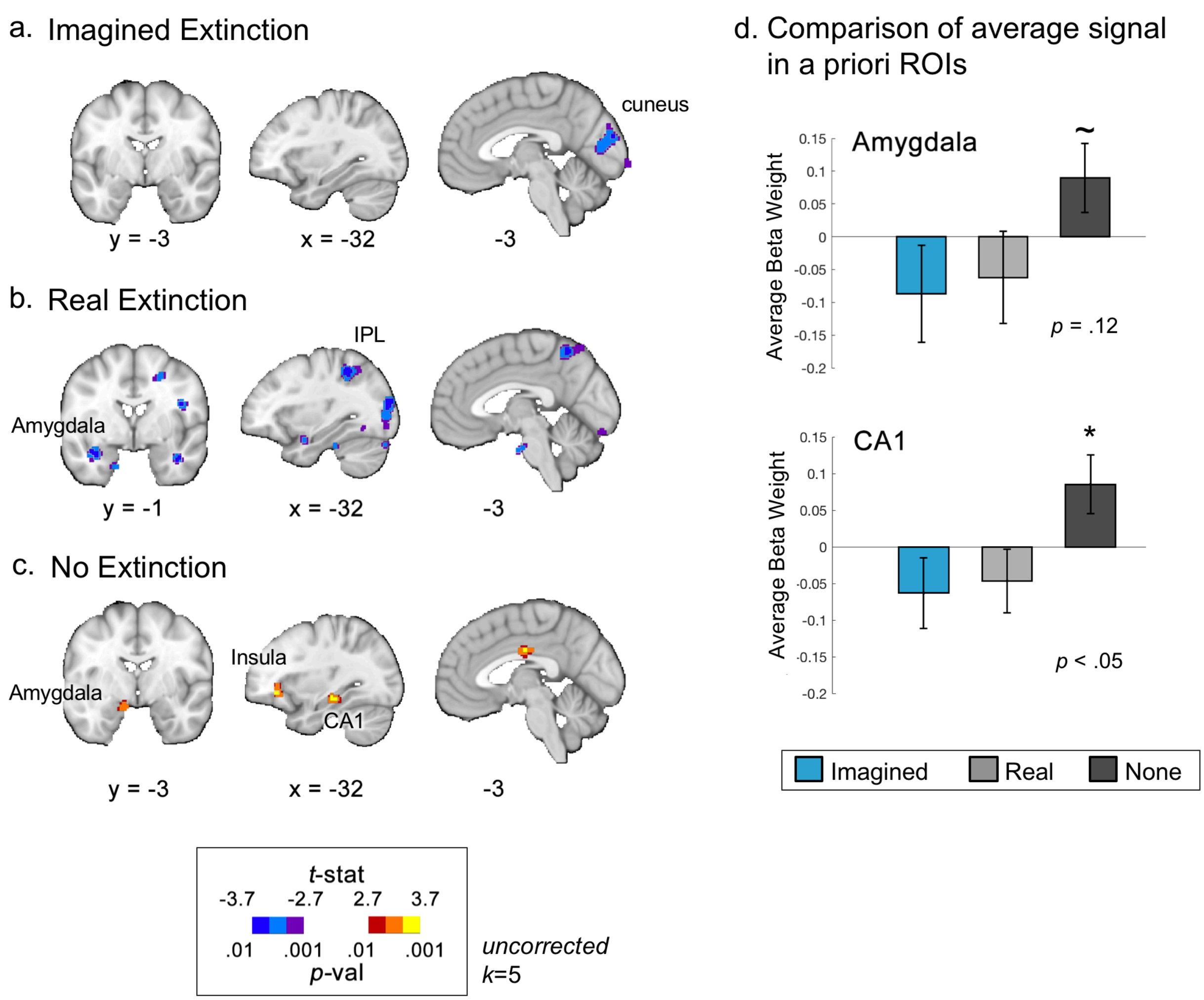

Supplementary Figure 3. Univariate Activation during Recovery Test (CS + > CS-), Related to Figure 3. A general linear model contrasting activation to the last 5 trials of re-extinction CS+ > CS- was applied across the whole brain within each group. Uncorrected t-statistics are plotted for each map ($P < 0.05$, cluster size $k = 5$; see Table S3 for complete list of activations). **A. Imagined Extinction**. Amongst the significant clusters was the cuneus, which was negatively activated to the CS+ relative to CS-. This map demonstrates no evidence for threat recovery in the Imagined Extinction group. **B. Real Extinction.** Activations were distributed and largely negative. Notably, there were decreased responses to the CS+ relative to the CS- in the amygdala and the Inferior Parietal Lobule (IPL). **C. No Extinction.** The no extinction group demonstrated distributed positive activations, that is, greater responding to the threatening relative to the safety stimulus, in several regions known to be involved in threat expression, including the amygdala, anterior insula, hippocampus (CA1), and cingulate cortex. **D. Comparison of average signal in a priori ROIs.**

Unthresholded beta-weights in bilateral a priori ROIs, the amygdala and CA1, were extracted and averaged from the maps in A-C and then compared across groups. A one-way ANOVA revealed a non-significant trend of group effects in the amygdala ($F(2,63) = 2.23$, p = 0.12, $\eta^2 = 0.07$). Pairwise differences, revealed by two-sample t-tests, were not significant, but demonstrate a trend that activation in the amygdala is greater in the no extinction group ($\underline{x}$ = 0.09, n = 24) than in the imagined $t(35.64) = 1.95$, p = 0.06, CI=[0.36 -0.01], Hedges g = 0.59) or real extinction groups ($t(39.77)$ = 1.734,p = 0.09, CI=[0.33, -0.03], Hedges g = 0.51). There was no difference between the imagined ($\underline{x}$ = -.09, n = 20) and real extinction ($\underline{x}$ = -0.06, n = 22) groups ($t(39.61) = -0.25$, p = 0.81, CI=[-0.23, 0.18], Hedges g = -0.07). A one-way ANOVA revealed group effects in the CA1 ($F(2,63) = 3.61$, p = 0.03, $\eta^2 = 0.10$). Pairwise t-tests revealed that activation in CA1 is greater in the no extinction group ($\underline{x}$ =0.09) than in the imagined ($t(38.86) = -2.38$, p = 0.02, CI=[-0.27, -0.02], Hedges g = -0.71) or real extinction groups (t(43.20) = -2.24, p = 0.03, CI=[-0.25, -0.01], Hedges g = -0.65). There was no difference between the imagined ($\underline{x}$ = -0.06) and real extinction ($\underline{x}$ = -0.04) groups ($t(39.13) = -0.25$,p = 0.80, CI=[-0.15, 0.11], Hedges g = -0.08).

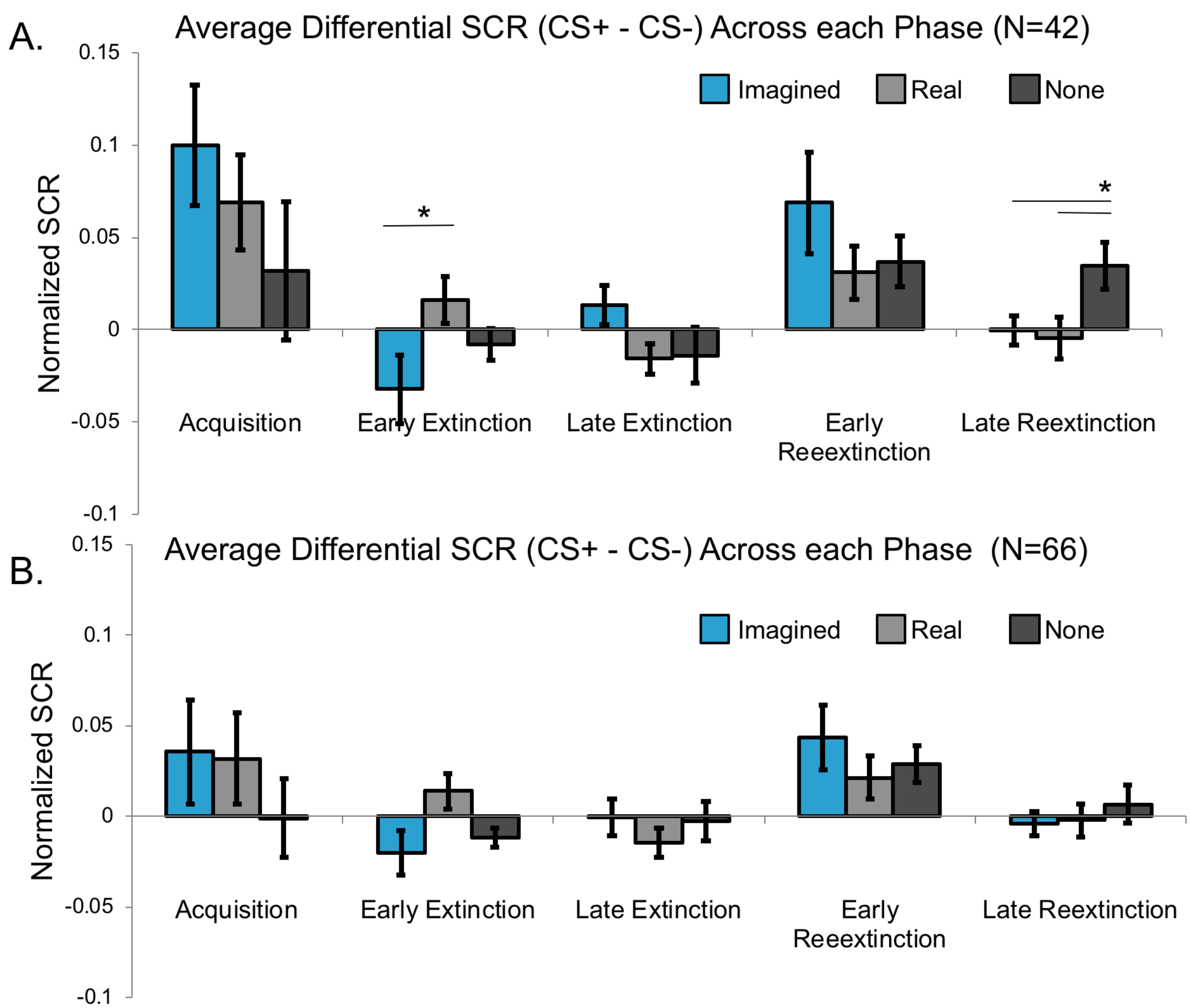

Supplementary Figure 4. Average skin conductance responses across all phases, Related to Figure 3. *A. Average Differential SCR Across Each Phase.* A linear mixed effects model including group and phase as predictors, indicated a significant effect of phase across the entire experiment ($F(4,156) = 9.19$, $P = 1.08\text{e-}06$). There was a trend towards a significant group by phase interaction ($F(8,156) = 1.78$, $P = 0.08$). The planned group comparison of threat-related SCRs during late re-extinction was significant and included in the main text. Post hoc analysis of group differences during early and late extinction phases revealed a significant group by phase interaction ($F(2,39) = 5.01$, $P = 0.01$) and a significant pairwise difference between imagined and real extinction groups during early extinction ($t(77.96) = -2.770$, $P = 0.02$; P value adjustment via tukey method for comparing a family of 3 estimates) Participants who did not demonstrate greater SCRs to the CS+ relative to the CS- on average across all acquisition trials (n = 24) were removed from analysis because it would be meaningless to investigate threat recovery in the signal of participants who did not demonstrate initial learning. *B. Average Differential SCR Across Each Phase for All Subjects (n = 66).* When participants who did not show a discriminatory SCR are not removed from the analysis, effects are diminished, but the trend remains. Additionally, this plot shows why it was necessary to remove participants who did not demonstrate a discriminatory SCR during learning; if there is no acquisition baseline it is difficult to assess the importance of recovery during late re-extinction.

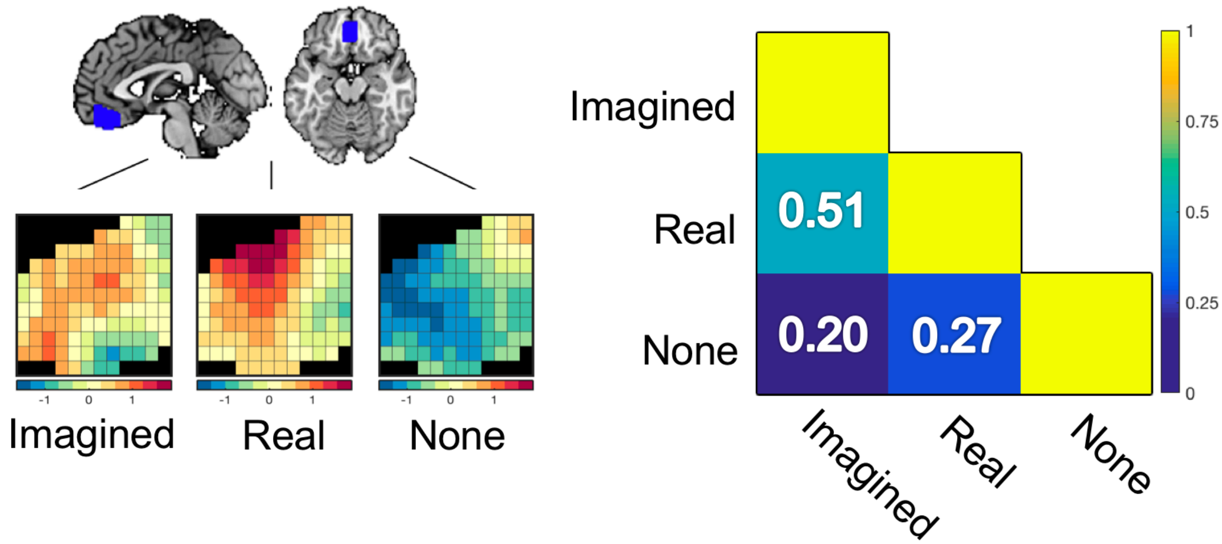

Supplementary Figure 5. Imagined and real extinction yield similar patterns in the vmPFC during extinction, Related to Figure 5. To assess the similarity of the representational content in the vmPFC across 'extinction' sessions, voxel-wise activations were tested for correlations between groups during extinction (the third time bin; Figure 4B). The third time bin was selected *post hoc*, based on the average temporal activation data in order to focus on the peak activation during extinction. Imagined and real extinction had the highest correlation coefficient (R = 0.51, P = 0.25.). Imagined and no extinction were weakly positively correlated (R = 0.20, P = 0.76) and real and no extinction were also weakly positively correlated (R = 0.27, P = 0.66). These correlations were not significant according to a nonparametric bootstrap test (10,000 samples). These results suggest that activations in the vmPFC are spatially analogous in imagined and real extinction, but require further data.

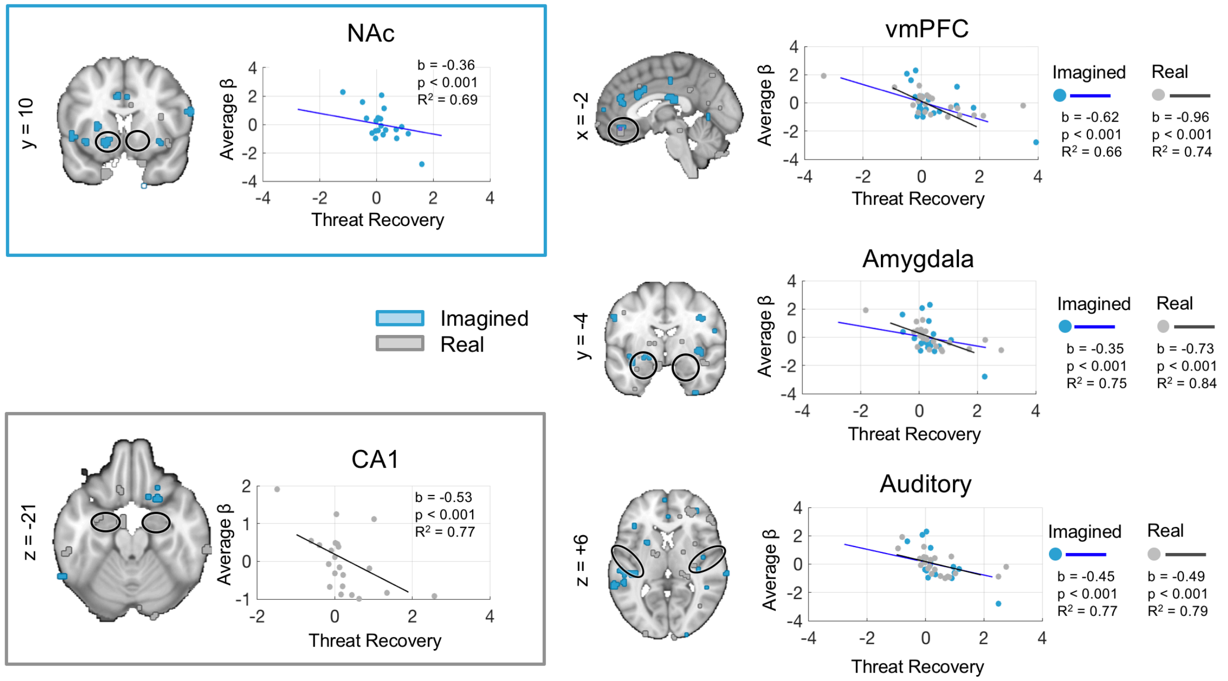

Supplementary Figure 6. Distribution of data supporting the effects in ROIs that predict the success of imagined and real extinction, Related to Figure 6. Scatterplots are shown for descriptive purposes. These plots illustrate the distribution of individual data values in Figure 6, but should not be taken as indicative of the true effect sizes (Reddan, Lindquist, & Wager, 2017).